이학석사 학위논문

Hepatocyte Growth Factor makes Human Mesenchymal Stem cells be rejuvenated by RAD51 pathway

간세포 성장 인자는 RAD51 경로로 인간 중간엽 줄기세포를 젊게 한다.

2015년 8월

서울대학교 대학원

분자의학 및 바이오제약전공

박종남

Abstract

Hepatocyte Growth Factor makes Human Mesenchymal Stem cells be rejuvenated by RAD51 pathway

- HGF from hE-MSCs rejuvenates hBM-MSCs -

JongNam Park

Molecular Medicine and Biopharmaceutical Sciences

WCU Graduate School of Convergence Science and Technology

The Graduate School Seoul National University

Human embryonic stem cell - derived mesenchymal stem cells (hE-MSCs) represent a better choice than adult stem cells (SCs) for cell-based therapy owing to their limitless capacity for self-renewal. We screened hE-MSCs and human bone marrow (hBM) - derived mesenchymal stem cells (MSCs) to identify secretory cytokines that were more strongly expressed in

hE-MSCs and could be used as additives to rejuvenate hMSCs in culture. We identified hepatocyte growth factor (HGF) as a candidate molecule through loss- and gain-of-function experiments in hE-MSCs and hBM-MSCs, respectively. Adding HGF to hBM-MSCs increased telomere length and induced OCT4 and Nanog expression. RAD51 was identified as a factor acting downstream of HGF to promote telomere elongation. OCT4 and Nanog were also upregulated by RAD51 overexpression and downregulated by *RAD51* RNA interference. To elucidate the mechanism underlying HGF-RAD51 signaling, we screened the putative *RAD51* promoter and identified transcription factor - binding sites for IKAROS family zinc finger (IKZF) and Runt-related transcription factor (RUNX)1. Knockdown of these two factors in hBM-MSCs in the presence of recombinant human HGF reduced telomere length as well as OCT4, Nanog, and RAD51 expression. Treatment of hMSCs with rhHGF had no adverse effects on cell viability, and chromosomal configuration was normal, as determined by G-band analysis and telomere fluorescence in situ hybridization. These results suggest that HGF treatment is a safe and effective means of increasing the self-renewal capacity of hMSCs in cell-based therapies.

Keywords: hE-MSCs, hBM-MSCs, HGF, RAD51, rejuvenator

Student Number: 2013-24032

Contents

List of Figures

Introduction

Preclinical and clinical studies of human bone marrow (hBM)-derived mesenchymal stem cells (MSCs) have demonstrated their ability to stimulate endogenous repair systems, suggesting their potential as a powerful tool for treating human disease (Parekkadan and Milwid, 2010). However, the finite capacity for self-renewal of hMSCs, including hBM-MSCs, limits their clinical application (Bertolo et al., 2013). In addition, the mechanisms controlling hMSC proliferation and senescence remain unclear (Fuchs and Chen, 2013).

It was recently reported that the upregulation of Oct4 and Nanog is associated with enhanced proliferation and differentiation potential in hMSCs (Huang et al., 2014; Tsai et al., 2012), demonstrating the importance of these factors in maintaining hMSC properties by suppressing spontaneous differentiation. Cell senescence is a complex process controlled by genetic and environmental variables; hMSCs cease to divide as a result of replicative senescence, which is elicited by progressive telomere shortening (Baxter et al., 2004; Stewart et al., 2003). Senescence of hMSCs is associated with a gradual loss of telomeric DNA due to telomerase inactivity (Kang et al., 2004; Shi et al., 2002; Simonsen et al., 2002; Takeuchi et al.,

2007).

Unlike hMSCs, embryonic stem cells (ESCs) derived from the inner cell mass of the blastocyst display infinite self-renewal capacity. Thus, human ESC - derived MSCs (hE-MSCs) are a self-replenishing source of cells that represent a better choice than adult stem cells for cell-based therapy. In our previous study, we demonstrated that hE-MSCs can be produced, maintained, and expanded more consistently and effectively than hMSCs (Lee et al., 2010). In the present study, we sought to characterize the mechanism underlying the maintenance of pluripotency in hE-MSCs and identify factors that can re-establish the stemness of hMSCs, as determined by OCT4 and Nanog expression and telomere length. We screened hE-MSCs and hBM-MSCs and identified hepatocyte growth factor (HGF) as being more strongly expressed in the former cell type, which we used as an additive in hBM-MSC cultures. We demonstrate that HGF overexpression induces an increase in telomere length and upregulation of OCT4 and Nanog expression in hMSCs via RAD51, suggesting that it can be used to enhance the efficacy of hBM-MSCs in cell-based therapies.

Materials and methods

hMSC culture and recombinant hHGF addition or hHGF neutralization

hE-MSCs (human embryonic stem cell derived mesenchymal stem cells) were cultured in EGMTM-2MV medium (Lonza, Basel, Switzerland) and hBM-MSCs (human bone marrow derived mesenchymal stem cells, Lonza) were grown in MSCGM medium (Lonza) at 37°C with 5% CO_2. In this study, we used hE-MSCs at passage 14 and hBM-MSCs at passage 7.

HGF neutralizing antibody (2.5 μg/mL Abcam, Cambridge, UK) was added to hE-MSCs (high HGF-hMSCs) to block HGF function every 8 h. Human Recombinant HGF (10 ng/mL R&D Systems, USA) was added to hBM-MSCs (low HGF hMSCs) every day for 5 days. Medium was exchanged daily with each addition of recombinant hHGF.

Real-time PCR analysis

QIAshredder and an RNeasy mini kit (Qiagen) were used to prepare total RNA according to manufacturer instructions. Subsequently, 1 μg RNA was transcribed to cDNA using the

PrimeScript 1st strand cDNA Synthesis kit (Takara, Tokyo, Japan). PCR was performed with Power SYBR Green PCR master mix (Applied Biosystems, Foster City, CA). Real-time samples were run on an ABI PRISM 7500 sequence detection system (Applied Biosystems). GAPDH was used as the internal control and for normalization.

The real-time PCR primers were as follows:
5′-GAGGCAACCTGGAGAATTTG-3′, Oct4, forward:
5′-TAGCCTGGGGTACCAAAATG-3′; Oct4, reverse:
5′-TTCCTTCCTCCATGGATCTG-3′, Nanog, forward:
5′-TGCTGGAGGCTGAGGTATTT-3′; Nanog, reverse:
5′-GCATAAATGCCAACGATGTG -3′, RAD51, forward:
5′-GTGGTGAAACCCATTGGAAC-3′; RAD51, reverse:
5′-GGATATTGTGGCCGAAGCTA-3′, IKZF1, forward:
5′-GTTTGGCGACGTTACTTGCT-3′; IKZF1, reverse:
5′-CGAAGACATCGGCAGAAACT-3′, RUNX1, forward:
5′-TGCCTTGTATCCTGCATCTG-3′; RUNX1, reverse:
5′-TGTGAGGAGGGGAGATTCA-3′, GAPDH, forward:
5′-CAACGAATTTGGCTACAGCA-3′.GAPDH reverse:

Western blot analysis

All hMSCs were lysed with protein lysis buffer (50 mmol/L Tris - HCl, 150 mmol/L NaCl, 1% NP 40, 0.1% sodium dodecyl

sulfate, and 0.5% deoxycholate) containing protease inhibitor cocktail (Roche, Indianapolis, IN). Total lysates (25 μg) were separated by sodium dodecyl sulfate - polyacrylamide gel electrophoresis and transferred by electro-blotting onto a PVDF membrane (Millipore, Billerica, MA). Membranes were incubated in primary antibody overnight at 4℃. Primary antibodies were as follows: anti-Oct4 antibody (1:2000; Santa Cruz Biotechnology, Santa Cruz, CA), anti-Nanog antibody (1:1000; Abcam), anti-RAD51 (1:500; Cell Signaling Technology, Davers, MA) and anti-TERT antibody (1:1000; Abcam). The α-tubulin antibody (1:5000; Sigma Aldrich, St. Louis, Missouri) was used as an internal housekeeping control. Then, the immunoblotted membranes were incubated with HRP-conjugated secondary antibodies (1:2000; Sigma Aldrich) for 2 h at room temperature. Quantitative analysis of immunoreactive bands was performed using ImageJ (NIH, Bethesda, MD) software program.

TRAP and HR assays

To detect telomerase activity, the TRAPEZE Telomerase Detection kit (EMD Millipore) was used. The DNA samples were separated by 12% DNA polyacrylamide gel electrophoresis. The polyacrylamide gels consisted of 40% acrylamide, TBE electrophoresis buffer, 10% APS, and TEMED.

The Homologous Recombination Assay kit (Norgen biotek, Ontario, Canada) was used to evaluate the efficiency of homologous recombination according to manufacturer instructions. PCR products were quantified by ImageJ analysis of the gel images (NIH, Bethesda, MD).

Quantitative real-time PCR for analysis of telomere length

Quantitative real-time PCR was used to evaluate telomere lengths according to Samsonraj et al. (Samsonraj et al., 2013). Reactions were performed on an ABI PRISM 7500 as follows: 40 cycles of 95℃ for 15 s, 54℃ for 2 min. For 36B4 PCR as a single copy gene, the program included 40 cycles of 40 cycles of 95℃ for 15 s, 58℃ for 1 min. Primer sequences for the telomere length and 36B4 gene were as follows:

Tel1: 5′-GGTTTTTGAGGGTGAGGGTGAGGGTGAGGGTGAGGGT-3′;

Tel2: 5′-TCCCGACTATCCCTATCCCTATCCCTATCCCTATCCCTA-3′;

36B4u: 5′-CAGCAAGTGGGAAGGTGTAATCC-3′;

36B4d: 5′-CCCATTCTATCATCAACGGGTACAA-3′.

FACS analysis

The human mesenchymal stem cells were washed with FACS DPBS buffer (GIBCO) containing 2.5% fetal bovine serum (GIBCO) and incubated for 30 min with PCNA antibodies conjugated to fluorescein isothiocyanate (FITC) (1:100; AbD Serotec, Hercules, CA) for fluorescence-activated cell sorting (FACS). At least 10^4events were analyzed on aFACS Calibursystem (BD Biosciences) with CellQuest software.

Loss of function and gain of function

Specific gene knockdown was achieved by mixing siRNA with Metafectene PRO (Biontex, M(Bioen, Germany). Before transfection, siRAD51, siIKZF1, and siRUNX1 (all Dharmacon, Lafayette, CO) and Metafectene PRO transfection reagent were diluted in cultured medium without FBS at room temperature. Then, combined the two solutions and incubated for 15 min at RT. After incubation, the RNA-transfection reagent complex was added dropwise to the culture dish. After 6 h incubation at 37℃ in a CO_2 incubator, the medium was exchanged with fresh culture medium.

A CMV-lentivirus for RAD51 overexpression was purchased from Sirion Biotech (Am Klopferspitz, Germany). The lentivirus

supernatant diluted with complete culture medium containing 1 μe/mL polybrene was added to the hMSCs culture plate. More than 1 × 10^7lentivirusparticles were added to each culture plate(50−60% cell confluency).

After24h,the medium was exchanged for fresh culture medium and incubated at 37℃ to allow growth of the virus-infected cells.

Human growth factor array and ELISA assay

Human growth factor array C1 (Raybiotech, Norcross, GA) was used to analyze the quantitative differences in secreted growth factors between hE-MSCs and hBM-MSCs. Cultured supernatants of hMSCs were processed according to manufacturer protocols. Imaging was performed with a Chemiluminescence Bioimage analyzer (Alpha Innotech, San Jose, CA)

To measure secreted HGF and IGFBP1, cell culture supernatants of hMSCs were analyzed by human HGF quantikine ELISA kit or human free IGFBP1 quantikine ELISA kit, (R&D Systems, Minneapolis, MN). Results were read on an ELISA reader, MultiskanTM GO Microplate Spectrophotometer (Thermo Scientific, Waltham, MA) at 450 nm.

G-band and telomere FISH

Cell division was blocked at mitotic metaphase by 0.1 g/mL colcemid (GIBCO-Invitrogen) for 2 h. Then, hBM-MSCs were trypsinized and resuspended in 0.075 M KCl for 20 min at 37℃. After incubation, the cells were fixed in a 3:1 ratio of cold methanol:acetic acid. G-band standard staining was used to visualize the chromosomes. When at least 20 cells were detected, karyotypes were analyzed and reported according to the International System for Human Cytogenetic Nomenclature.

For telomere FISH, mitotic cells were collected by mitotic shake-off and swollen in hypotonic solution (0.075M KCl) at 37 °C for 20min. Then, cells were fixed in a freshly prepared 3:1 mix of methanol:glacial acetic acid, glacial. Fixed cells were dropped onto pre-cleaned slides and left to dry overnight. FISH was performed as described manufacturer's instructions (Cellay). In briefly, the slides were hybridized with Pan-Telomere OligoFISH probes (Cellay) and incubated for 10 minutes at 37 °C. The slides were washed in 2xSSC under agitation to float off the coverslip and then incubated in IsoThermal Wash Solution (Cellay) for 5 minutes at room temperature. Finally the slides were rinsed in 2xSSC and mounted with Antifade with DAPI and analyzed with fluorescence microscope.

Immunocytochemistry

Cultured hMSCs were fixed with acetone for 3 min at -20℃ and washed three times with 1× PBS (phosphate buffer saline) buffer. Unspecific binding was blocked with 0.1% bovine serum albumin and 0.05% Triton-X-100 in DPBS (GIBCO) for 1 h. Subsequently, hMSCs were incubated overnight at 4°. Subsequently, hMSCs were incubated overnight a) and erica, (1:200, Millipore). After three 5-min washes, the cells were incubated with secondary antibodies conjugated to Alexa Fluor fluorescent dyes (1:200; Invitrogen) for 2 h at RT. Images were obtained by confocal microscopy (Carl Zeiss LSM710, Germany).

Ultraviolet (UV) irradiation was performed for 2 h under the UV lamp of a clean bench (100 - 180 nm).

Mouse liver fibrosis model and cell transplantation

This study was approved by the institutional review board of Seoul National University Hospital. Animal experiments were approved by the Institutional Animal Care and Use Committee (IACUC) of Seoul National University Hospital, Korea. BALB/c-nude mice (male, 12 - 13 weeks old, 20 - 25 g) were used for all animal experiments. Mice were given TAA (thioacetamide, 200 mg/kg) (Sigma Aldrich) by intraperitoneal

injection three times per week for 14 days. The negative control group was injected with 0.9% saline. Cell transplantation was performed by intracardiac injection at 0day after the first TAA (see Figure 7A). Normal mice in the negative control group and mice in the positive control group injected with TAA were given DPBS. Mice in the cell transplantation groups were administered BM-MSCs or BM-MSCs treated with 10 ng/mL rhHGF for 5 days. After a 2-d recovery period, mice were injected with TAA three times a week until the 14th day after transplantation.

BM-MSCs stained with CellTracker CM-DiI (Invitrogen) were injected into the mice for cell tracking in liver tissue. CellTracker CM-DiI (4 μg/mL) was used to stain the cells at 37℃ for 24 h. On day 14 after cell transplantation, liver tissues were harvested for histology.

Statistical analysis

Statistical comparisons were conducted using GraphPad Prism 6 (GraphPad Software, La Jolla, CA). Quantitative data were reported as the mean ± SEM and unpaired t-test analysis of variance was used to analyze each group. P-values < 0.05 were regarded as statistically meaningful.

Results

hE-MSCs have higher proliferative capacity than hB-MSCs

To assess proliferative capacity, we performed fluorescence-activated cell sorting (FACS) analysis with the S phase-specific marker proliferating cell nuclear antigen (PCNA) and found a greater proportion of hE-MSCs than hBM-MSCs in the S phase (28.85% ± 3.77% vs. 6.42% ± 0.43%; Fig. 1A). Additionally, the stemness factors OCT4 and Nanog were more highly expressed (Fig. 1B) and telomere length was significantly longer (Fig. 1C) in hE-MSCs than in hBM-MSCs.

Hepatocyte growth factor (HGF) modulates telomere length and stemness

To identify the factor that is responsible for maintaining SC identity in hE-MSCs and could potentially be used to rejuvenate hMSCs, we carried out a screen for secretory cytokines highly expressed in hE-MSCs and identified two candidates, HGF and insulin-like growth factor-binding protein (IGFBP)1 (Fig. 2A). An enzyme-linked immunosorbent assay (ELISA) confirmed that both proteins, but especially HGF, were expressed at higher levels in hE-MSCs than in hBM-MSCs (Fig. 2B). To verify the role of

HGF in the regulation of telomere length and stemness maintenance, we used hE-MSCs and hBM-MSCs as models for high and low HGF expression, respectively. Endogenous HGF function was blocked in hE-MSCs with a neutralizing antibody, resulting in a decrease in telomere length and proliferative capacity (Fig. 2C). Conversely, adding recombinant human (rh)HGF to hBM-MSC cultures increased telomere length and induced proliferation (Fig. 2D) and enhanced OCT4 and Nanog expression (Fig. 2E).

HGF modulates telomere length via RAD51

To investigate the mechanism by which HGF modulates telomere length, we examined the expression of RAD51 and telomerase reverse transcriptase (TERT), two mediators of telomere elongation and maintenance in cancer and stem cells . TERT activity and expression were similar between hE-MSCs and hBM-MSCs (Fig. 3A). However, blocking RAD51 caused a decrease in RAD51 expression in hE-MSCs (Fig. 3B), whereas rhHGF treatment induced RAD51 upregulation in hBM-MSCs (Fig. 3C), with no changes observed in TERT levels (Fig. 3B, C). To confirm the HGF dependency of RAD51 activity, we performed a homologous recombination (HR) assay and found that rhHGF treatment increased RAD51 activity in hBM-MSCs to the level observed

in hE-MSCs (Fig. 3D).

RAD51 acts as a mediator between HGF and OCT4/Nanog in telomere regulation

To determine whether RAD51 plays a role in the regulation of telomere length and OCT4/Nanog expression by HGF, we inhibited *RAD51* expression in hBM-MSCs using short interfering (si)RNAs in the presence of rhHGF. RAD51 mRNA and protein levels increased in the presence of HGF and decreased upon siRNA-induced knockdown of *RAD51* (Fig. 4A, B); the latter also resulted in reduction in telomere length in the presence of HGF (Fig. 4C). OCT4 and Nanog protein levels were upregulated upon HGF treatment and downregulated by *RAD51* knockdown even in the presence of HGF (Fig. 4D). Restoring RAD51 expression with a lentiviral vector in the absence of rhHGF increased OCT4 and Nanog protein levels in hBM-MSCs (Fig. 4E).

HGF induces RAD51 expression via IKAROS family zinc finger (IKZF)1 and Runt-related transcription factor (RUNX)1

We searched for transcription factors that mediate the effects of

HGF on RAD51. We identified four alternative transcripts of *RAD51* on chromosome 15 and mapped a putative promoter region spanning ~2.3 kb (Supplementary Fig. 2A). The candidate factors IKZF1 and RUNX1 were identified from transcription factor binding site analysis (TFSEARCH v1.3 database) (Supplementary Fig. 2B); to assess their function, we performed knockdown experiments in hBM-MSCs treated with rhHGF. In the presence of rhHGF, RAD51 mRNA and protein levels were upregulated; however, this effect was abolished when *IKZF1* or *RUNX1* was silenced by siRNA transfection (Fig. 5A, B). Moreover, telomere length was reduced and OCT4 and Nanog expression was downregulated in *IKZF1* or *RUNX1* knockdown cells (Fig. 5C, D). To determine the role of IKZF1 and RUNX1 in HGF function, the expression of these two transcription factors was inhibited in hE-MSCs (Fig. 5E), resulting in the downregulation of *RAD51* mRNA (Fig. 5F) and protein (Fig. 5G) and decrease in telomere length (Fig. 5H).

RAD51 mediates telomere regulation by HGF

To investigate the possibility that RAD51 upregulation was the result of DNA double-strand breaks (DSBs) induced by exogenous rhHGF treatment, we examined whether DSBs were generated in hBM-MSCs treated with rhHGF by immunocytochemical analysis of γ-H2AX expression. The level of

RAD51 was increased by ultraviolet (UV) irradiation (control) and in the presence of rhHGF; however, while irradiated cells were positive for γ-H2AX, no immunoreactivity was observed in rhHGF-treated hBM-MSCs (Fig. 6A). We also examined chromosomal stability with the G-band assay and telomere fluorescence in situ hybridization (FISH) after rhHGF treatment. The karyotyping results and G-band analysis showed normal chromosomes with no detectable translocations (Fig. 6B); however, telomere FISH revealed abnormal telomere status, including telomere fusion, although extra-telomeric signals were not observed (Fig. 6B).

HGF treatment enhances the therapeutic efficacy of hBM-MSCs

To evaluate the therapeutic potential of hBM-MSCs, the cells were treated with rhHGF and transplanted into mice with thioacetamide (TAA)-induced liver fibrosis (Fig. 7A). Histological analysis involving Masson's trichrome staining to detect collagen fibers revealed an accelerated recovery and regression of surface undulations of TAA-induced liver lesions on day 14 in mice transplanted with rhHGF-treated hBM-MSCs as compared to the findings for untreated hBM-MSCs (Fig. 7B). Collagen deposits were visualized and quantified by Picrosirius Red staining, which detects type I and III collagen. The transplantation of

rhHGF-treated hBM-MSCs inhibited portal-to-portal bridging and septum formation as compared to that seen in PBS-treated hBM-MSC controls and was associated with decrease in fibrotic area (Fig. 7C), indicating that the therapeutic effects of hBM-MSCs were enhanced by pretreatment with HGF.

Discussion

HGF regulates telomere length and OCT4 and Nanog expression via RAD51 in hMSCs

Spontaneous telomere elongation/maintenance is common in cancer cells and is targeted by therapeutic agents for cancer treatment (Lu et al., 2014). While telomere elongation/maintenance is also desirable in stem cells used for regenerative medicine (Shi et al., 2002; Simonsen et al., 2002), it is achieved by genetic modification, for instance by introducing hTERT, which can activate the c-myc oncogene in human mammary epithelial cells and must therefore be used with caution in therapeutic applications (Wang et al., 2000). In this study, we found that exogenously applied HGF increased telomere length in hBM-MSCs without inducing genetic modifications. Although increased telomerase activity by the addition of HGF has been reported in primary hepatocyte cultures (Inui et al., 2002), this is the first report of RAD51 acting downstream of HGF and inducing telomere elongation and increased expression of stemness factors.

Alternative role for RAD51 in hMSCs

DNA DSBs can be induced by external sources—including exposure to UV or ionizing radiation or environmental toxins—or by endogenous sources (Price and D'Andrea, 2013). Several DNA repair pathways exist that deal with each type of DNA damage; one example is HR, which is an error-free mechanism that maintains genomic integrity and ensures genetic variation (Aguilera and Gomez-Gonzalez, 2008). RAD51 is a RecA recombinase that has the essential role of loading DNA repair machinery at DSB sites during HR (Filippo et al., 2008; Kim et al., 2012). The formation of γ-H2AX foci is critical for an efficient DNA damage response; however, these were not observed in rhHGF-treated hBM-MSCs, indicating that the upregulation of RAD51 in the presence of HGF was not triggered by DNA damage.

The function of OCT4 and Nanog in MSCs is to maintain an undifferentiated, self-renewing state (Tsai et al., 2012). RAD51 induced an increase in OCT4 and Nanog levels in this study, although the underlying mechanism and the epigenetic effect on telomeres remain to be investigated. Nonetheless, we propose that RAD51 upregulation by HGF contributes to the rejuvenation of hMSCs by inducing telomere elongation and expression of the stemness factors OCT4 and Nanog.

IKZF1 and RUNX1 are novel transcriptional activators of RAD51

IKZF1 plays a role in lymphocyte development and homeostasis (Yoshida et al., 2013), while RUNX1 is essential for hematopoiesis as well as MSC proliferation and cell fate determination in myofibroblast differentiation (Kim et al., 2014; Lacaud et al., 2002). RAD51 expression is regulated by the transcription factors E26 transformation-specific 1/polyomavirus enhancer activator 3, E2F1, p53, epidermal growth factor receptor 1, and signal transducer and activator of transcription 5 (Hasselbach et al., 2005). We identified IKZF1 and RUNX1 as candidate transcription factors mediating the HGF-RAD51 axis by screening the ~2.3-kb putative promoter region of RAD51. Three transcripts shared the same transcription start site that included exons 1 and 3, while another had a different start site that included exon 2 and started 51 bp upstream of exon 1. We demonstrated that IKZF1 and RUNX1 function as transcriptional activators of RAD51 in hMSCs. Suppressing their expression in rhHGF-treated hBM-MSCs by RNA interference resulted in the downregulation of RAD51 as well as of OCT4 and Nanog expression, which was accompanied by telomere shortening; the same was observed in hE-MSCs in the absence of rhHGF. These results demonstrate that IKZF1 and RUNX1 are transcriptional activators of RAD51 in hMSCs.

Safety and therapeutic efficacy of HGF treatment

The upregulation of RAD51 is correlated with cancer cell survival and metastasis and poor prognosis. RAD51 mRNA and protein expression levels increase by approximately 4- and 6-fold, respectively, in cancer cells (Hine et al., 2008). We observed a < 2-fold increase in RAD51 expression in rhHGF-treated hBM-MSCs as compared to that in naïve cells. This led us to examine the therapeutic potential of HGF-rejuvenated hMSCs in a mouse model of liver fibrosis. There have been many advances in the development of antifibrotic therapies, but their safety and efficacy in humans have not been demonstrated (Bataller and Brenner, 2005). We investigated whether HGF can be useful for liver regeneration, given its role as a hepatocyte growth factor. The histological analysis revealed a significant reduction in fibrosis in mice transplanted with HGF-treated hBM-MSCs as compared to those transplanted with PBS-treated or untreated hBM-MSCs, and ectopic mass formation was not observed in other organs, suggesting that metastasis had not occurred. Our previous study showed that the minimum effective cell dose is 1 × 10^5perrat(Lee et al., 2012); given that rats weigh approximately 10 times more than mice, we transplanted a relatively high number of cells (5 × 10^4cellspermouse). Although the optimal cell dose in mice has yet to be determined, this enabled us to evaluate the efficacy, engraftment potential, and safety of

HGF-treated hBM-MSCs. Our findings demonstrate that HGF treatment is a safe and effective mean so increasing that herapeutic potential of hMSCs.

Figures

Figure 1A.

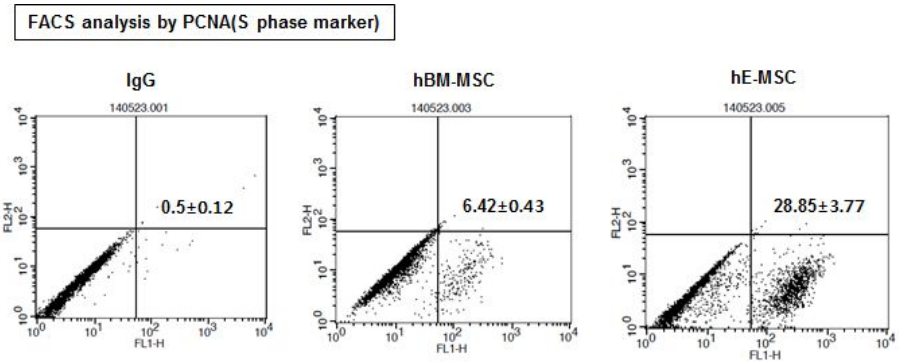

Figure 1B.

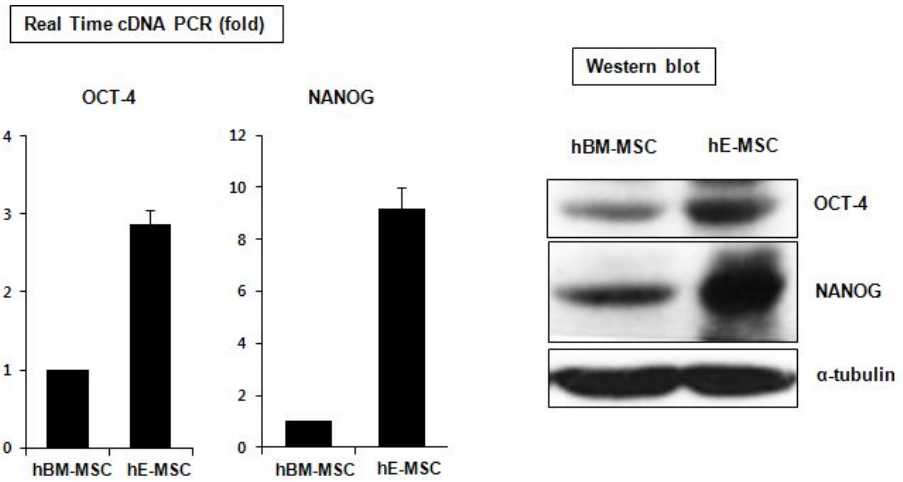

Figure 1C.

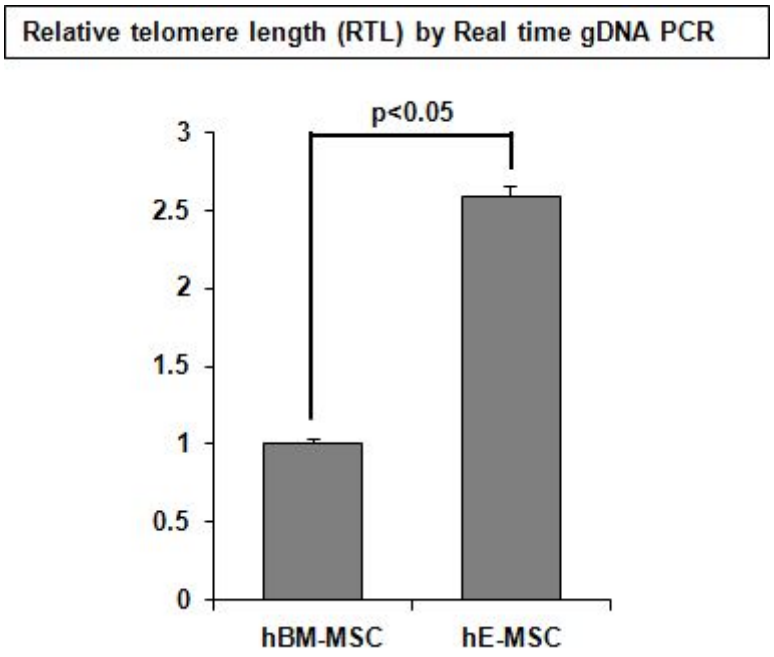
Relative telomere length (RTL) by Real time gDNA PCR
p<0.05
3
2.5
2
1.5
1
0.5
0
hBM-MSC
hE-MSC

Figure 1. Comparison of proliferative ability & stemness in hE-MSCs and hBM-MSCs.

(A) FACS analysis using the S phase marker PCNA showed greater expression in hE-MSCs than in hBM-MSCs.

(B) Real-time PCR cDNA amplification showed stronger expression of OCT4 and Nanog in hE-MSCs than in hBM-MSCs. Western blotting results were consistent with this finding.

(C) Comparison of telomere length. Relative telomere length (RTL) by real-time gDNA PCR represented longer telomeres in hE-MSCs than in BM-MSCs.

Figure 2A.

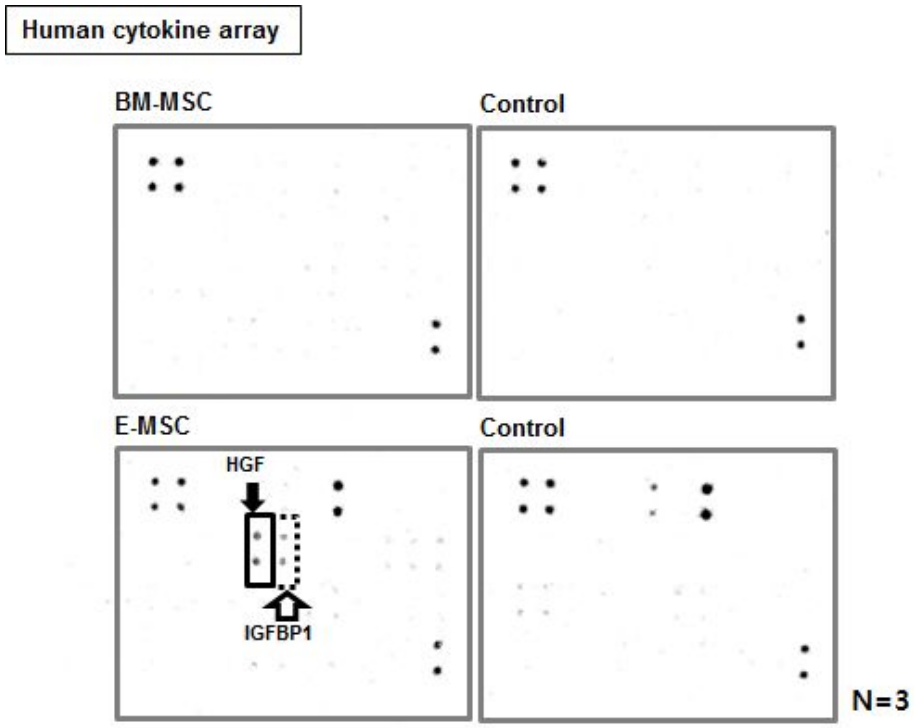
Human cytokine array
BM-MSC
Control
E-MSC
Control
HGF
IGFBP1
N=3

Figure 2B.

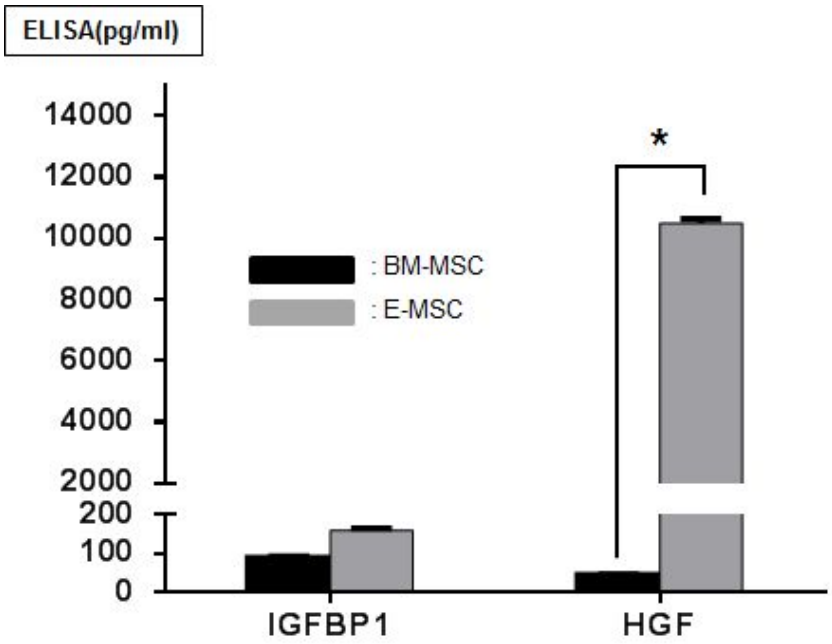

Figure 2C.

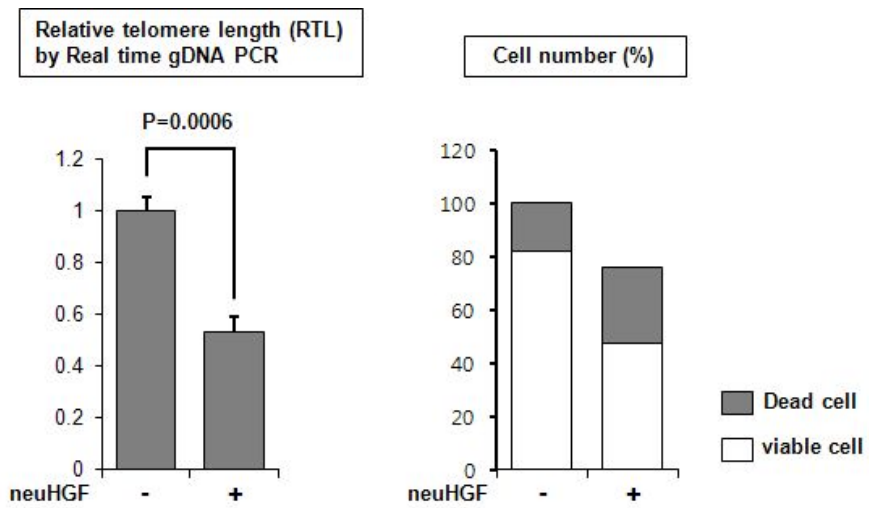

Figure 2D.

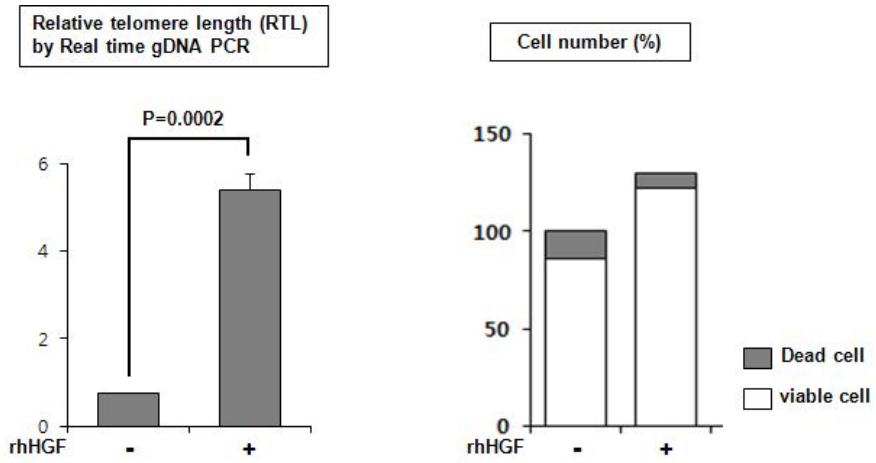
Relative telomere length (RTL)
by Real time gDNA PCR
P=0.0002
6
4
2
0
rhHGF
-
+
Cell number (%)
150
100
50
0
rhHGF
-
+
Dead cell
viable cell

Figure 2E.

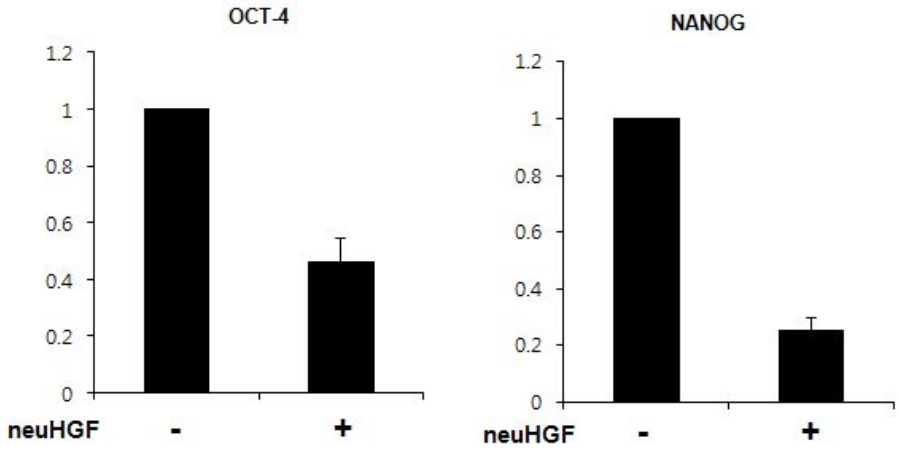

Figure 2F.

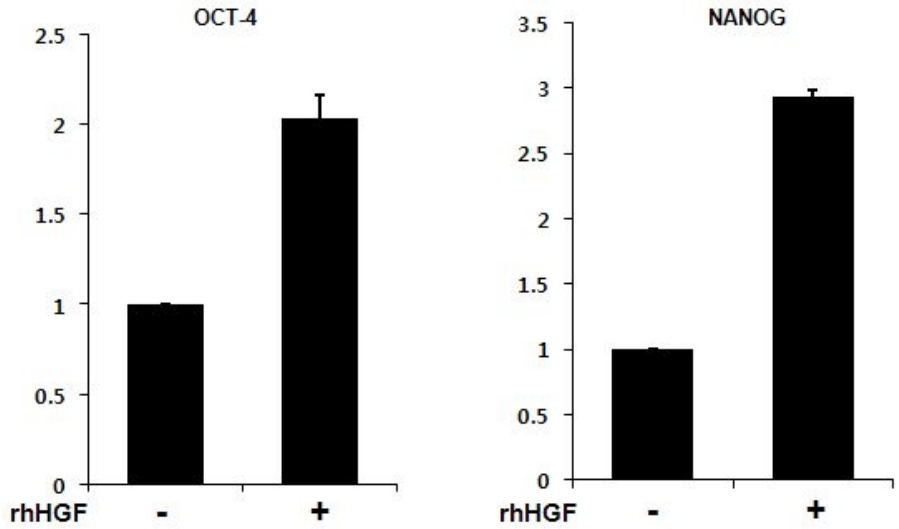

Figure 2. Screening of telomere and stemness regulator.

(A) Human cytokine array. Larger amounts of HGF and IGFBP1 were detected in hE-MSCs than in hBM-MSCs.

(B) ELISA. HGF expression was significantly greater in hE-MSCs than in hBM-MSCs, but there was little difference in IGFBP1.

(C) Loss-of function of HGF from hE-MSCs. After neutralizing HGF, decreasing telomere lengths and cell numbers were observed.

(D) Gain-of function of HGF in hBM-MSCs. Addition of rhHGF increased telomere lengths and cell numbers.

(E) Loss-of function of HGF from hE-MSCs. After neutralizing HGFm decreasing OCT4 and Nanog mRNA were observed.

(F) Upregulation of OCT4 and Nanog mRNA was observed in rhHGF-treated hBM-MSCs.

FIgure 3A.

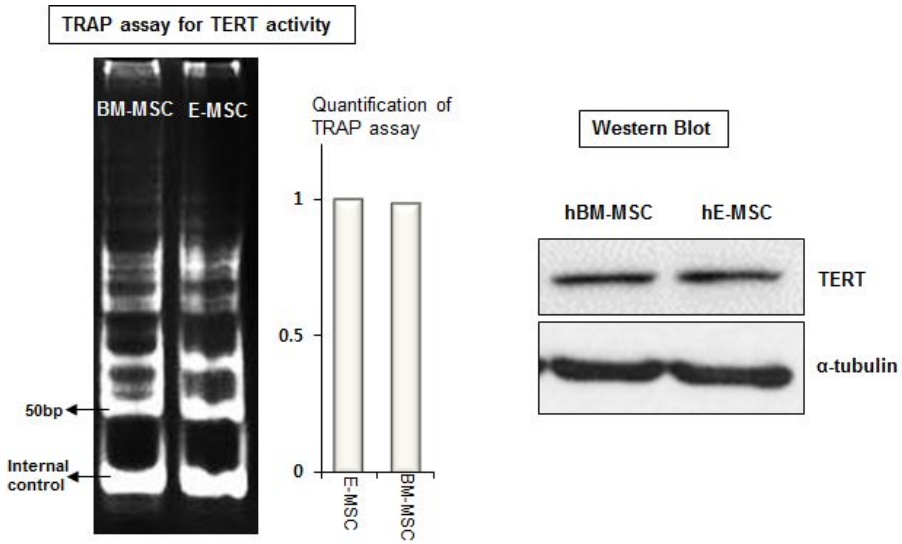

Figure 3B.

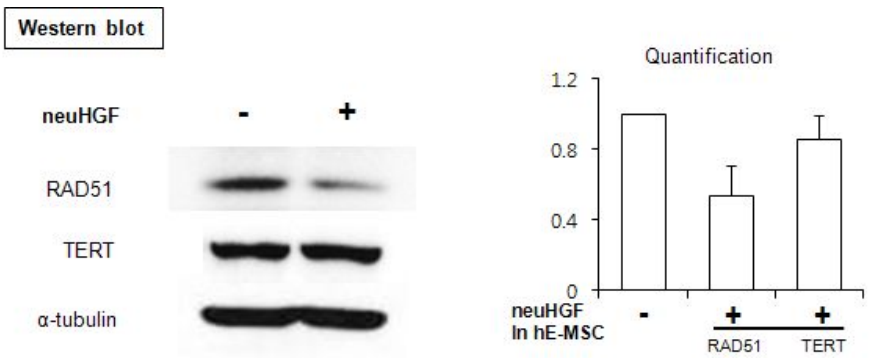

Figure 3C.

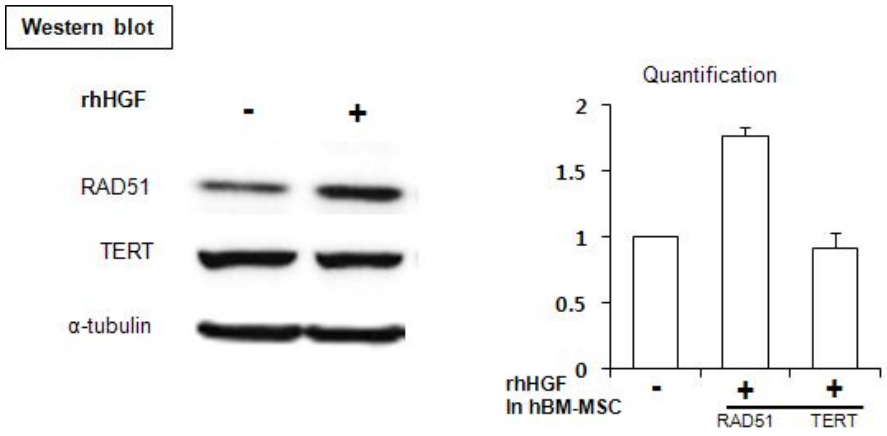

Figure 3D.

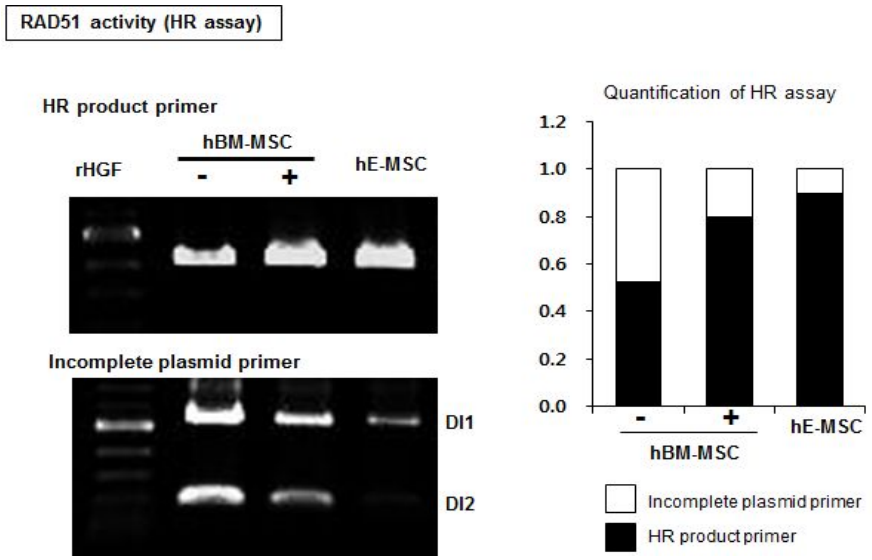

Figure 3. Development of RAD51 as a mediator between HGF-telomere.

(A) TRAP assay for TERT activity. There was no significant difference in TERT activity and expression of TERT protein between hE-MSCs and hBM-MSCs.

(B) Detection of RAD51 and TERT protein in HGF-neutralized HGF-treated hE-MSCs. RAD51 protein decreased but there was no effect on TERT.

(C) Detection of RAD51 and TERT protein in rhHGF-treated hBM-MSCs. rhHGF increased expression of RAD51 but produced no change in TERT protein.

(D) HR assay for RAD51 activity. RAD51 activity was upregulated by rhHGF in hBM-MSCs, similar to its activity in hE-MSCs. High-density HR product represents high HR activity. High density in incomplete plasmid primer was showed low activity in HR of RAD51.

Figure 4A.

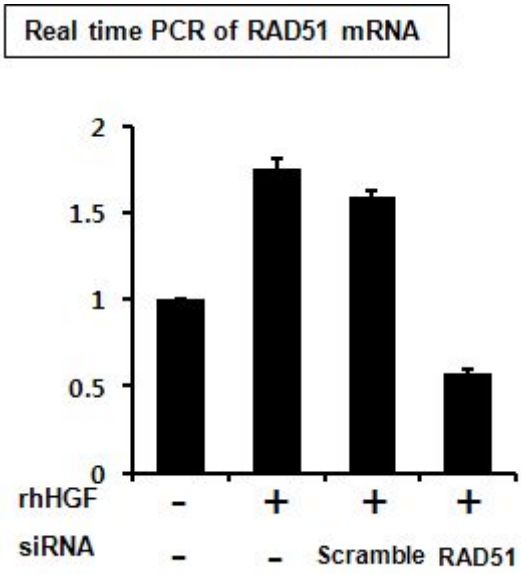
Real time PCR of RAD51 mRNA
2
1.5
1
0.5
0
rhHGF
siRNA
-
+
+
+
-
-
Scramble
RAD51

Figure 4B.

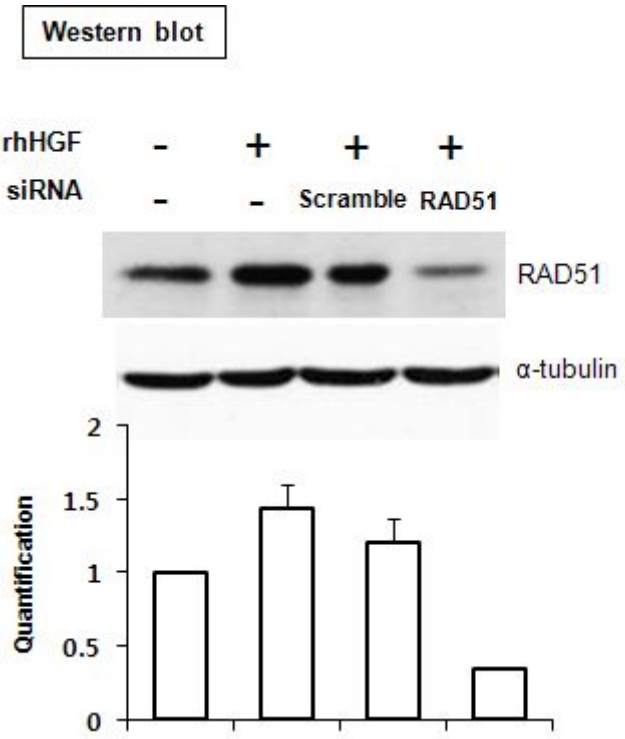
Western blot
rhHGF - + + +
siRNA - - Scramble RAD51
RAD51
α-tubulin
Quantification
2
1.5
1
0.5
0

Figure 4C.

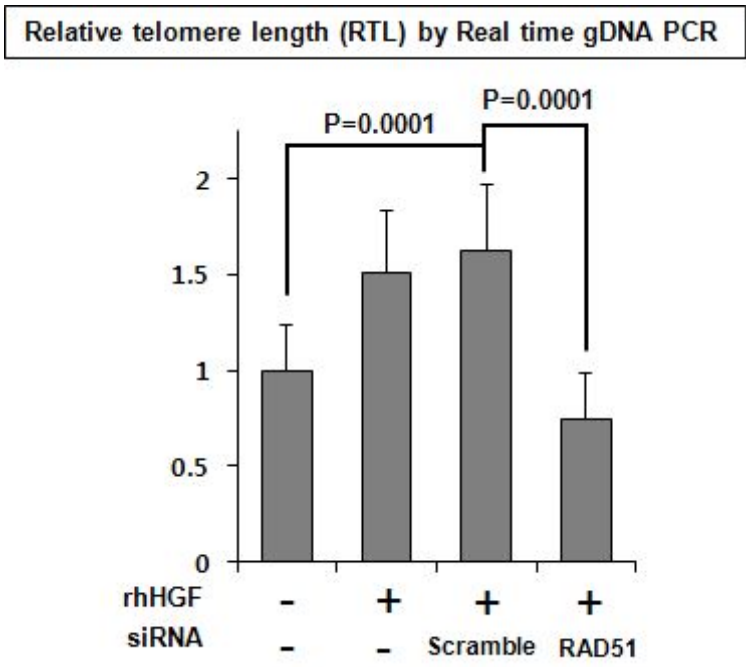
Relative telomere length (RTL) by Real time gDNA PCR
P=0.0001
P=0.0001
2
1.5
1
0.5
0
rhHGF
siRNA
-
+
+
+
-
-
Scramble
RAD51

Figure 4D.

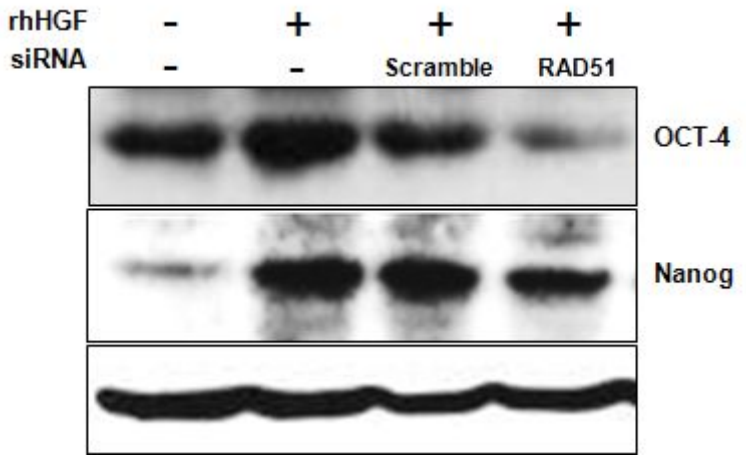

Figure 4E.

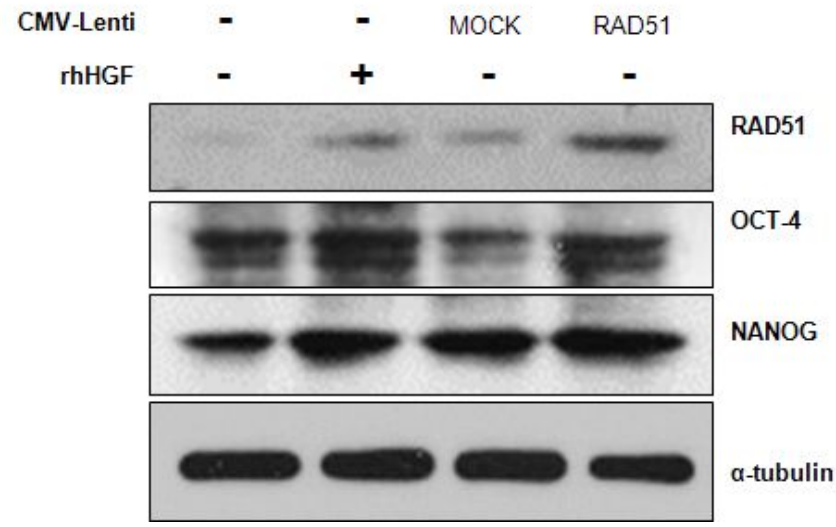

Figure 4. Confirmation of RAD51 as a mediator between HGF-Telomere/OCT4/Nanog.

(A-D) Loss-of-function of RAD51 in hBM-MSCs treated with rhHGF.

(A) Real-time PCR showed upregulation of RAD51 in the presence of rhHGF and downregulation by RAD51 siRNA.

(B) Western blot. Expression of RAD51 protein increased with rhHGF and was abrogated by RAD51 siRNA.

(C) RTL by real time gDNA PCR. RTL increased with rhHGF and decreased with RAD51 siRNA.

(D) OCT4 and Nanog protein expression was upregulated with rhHGF and downregulated by RAD51 siRNA.

(E) Western blot. RAD51 overexpression using CMV-Lentiviral vector showed upregulation of OCT4 and Nanog, similar to the results after rhHGF treatment.

Figure 5A.

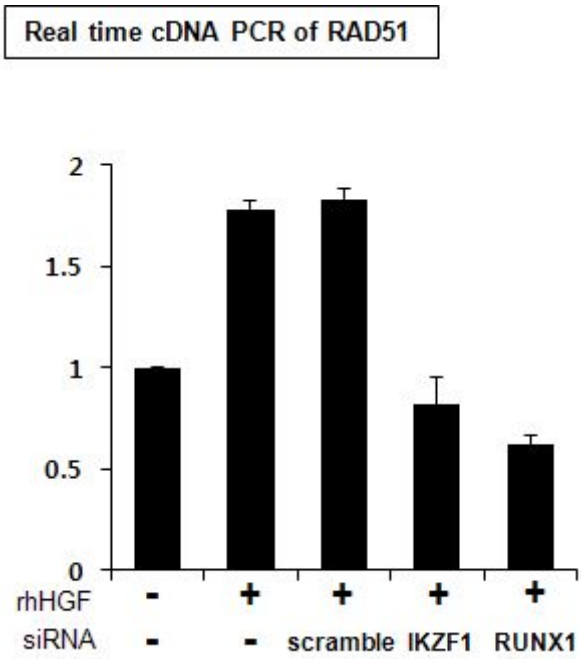

Figure 5B.

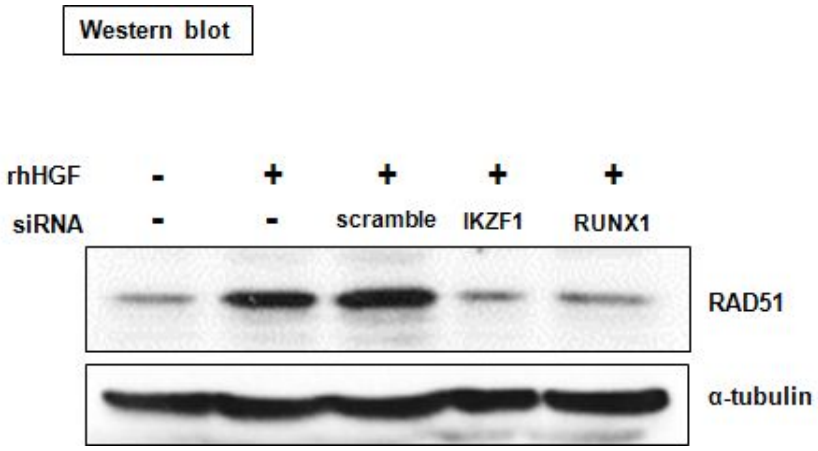

Figure 5C.

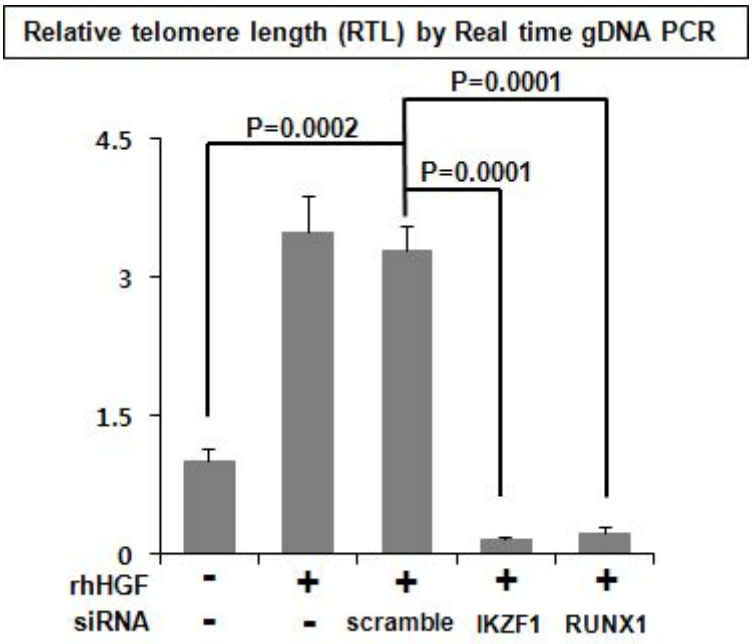

Figure 5D.

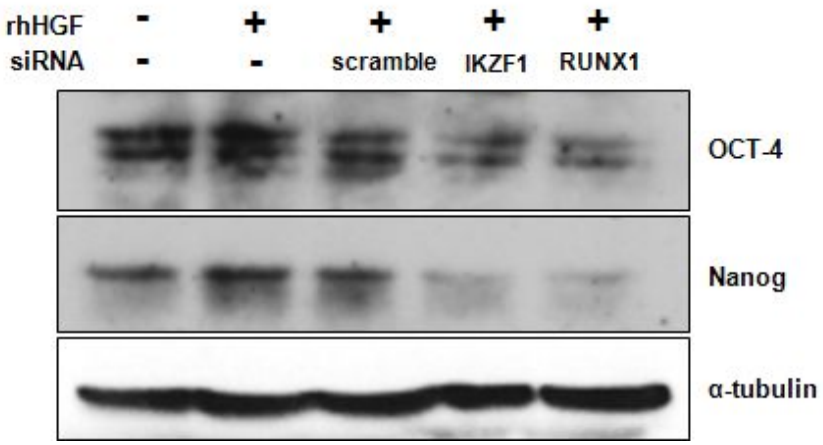

Figure 5E.

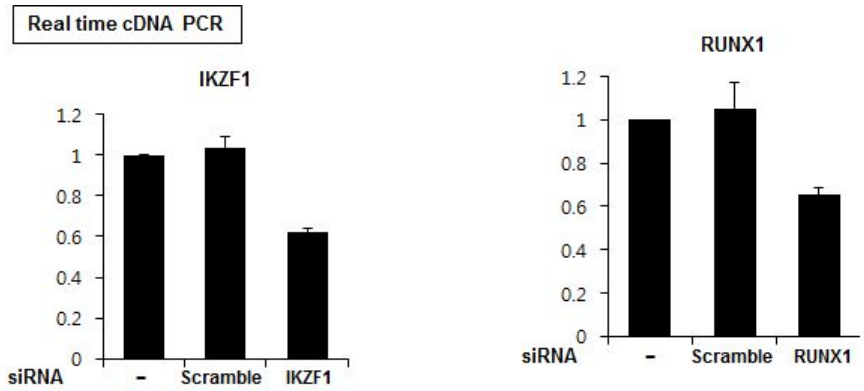

Figure 5F.

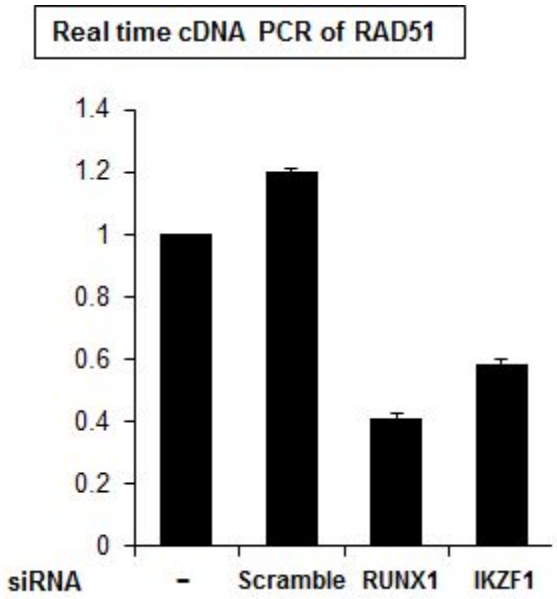

Figure 5G.

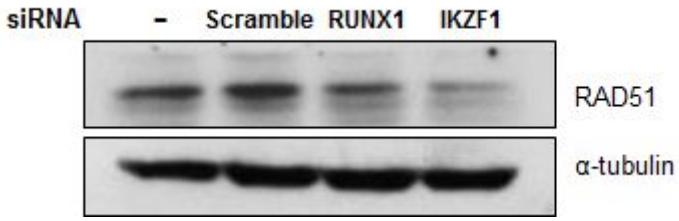

Figure 5H.

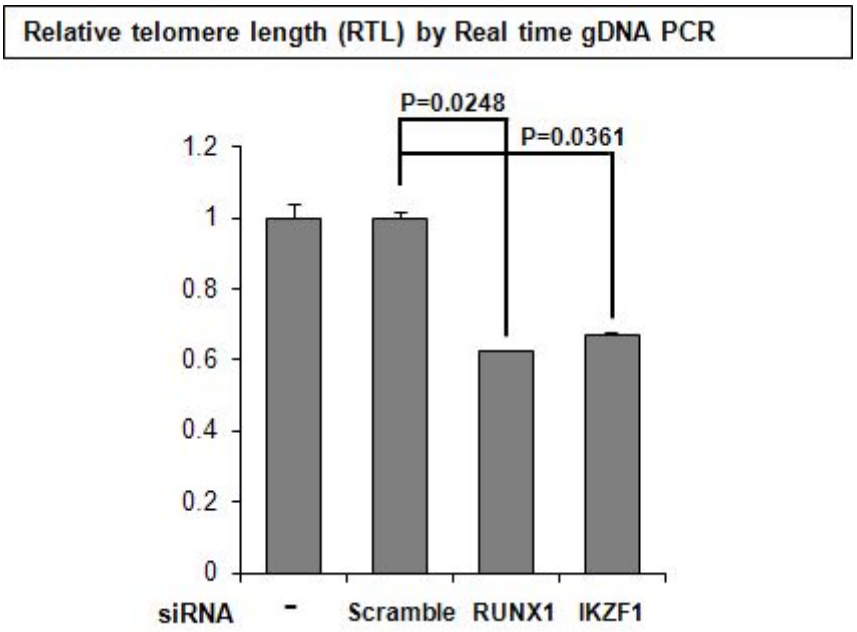

Figure 5. Confirmation of RAD51 transcriptional activators IKZF1 and RUNX1.

(A) Real-time cDNA PCR. RAD51 mRNA was downregulated by IKZF1 or RUNX1 knockdown, even in the presence of rhHGF.

(B) Western blot. Upregulated RAD51 protein in the presence of rhHGF was reduced by IKZF1 or RUNX1 siRNA.

(C) RTL by real time gDNA PCR showed the knockdown of IKZF1 or RUNX1 correlated with RAD51 downregulation.

(D) Western blot. Upregulated OCT4 and Nanog protein in the presence of rhHGF was abrogated by knockdown of IKZF1 or RUNX1.

(E-H) The relevance of IKZF1 or RUNX1 in hE-MSCs.

(E) Real-time cDNA PCR. Downregulation of IKZF1 or RUNX1 by siRNA was observed.

(F) RAD51 mRNA downregulation was detected in IKZF1 or RUNX1 knocked-down conditions

(G) Western blot. Expression of RAD51 protein was downregulated in IKZF1 or RUNX1 knocked down conditions.

(H) RTL by real-time gDNA PCR also showed a decrease under the same conditions.

Figure 6A.

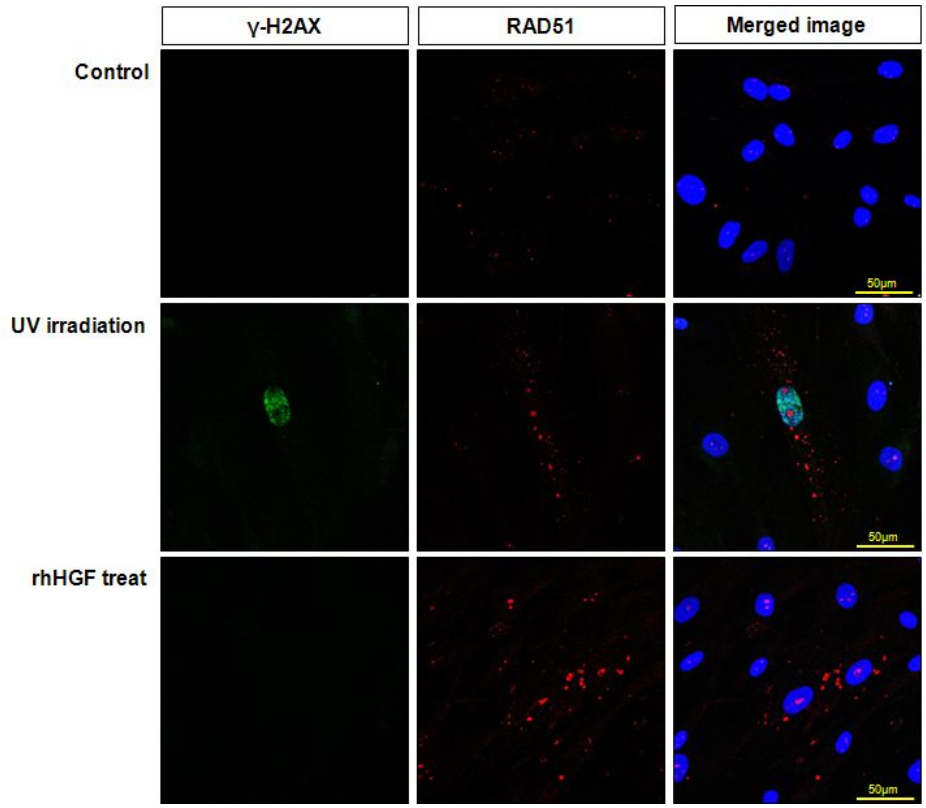
γ-H2AX
RAD51
Merged image
Control
UV irradiation
rhHGF treat
50μm
50μm
50μm

Figure 6B.

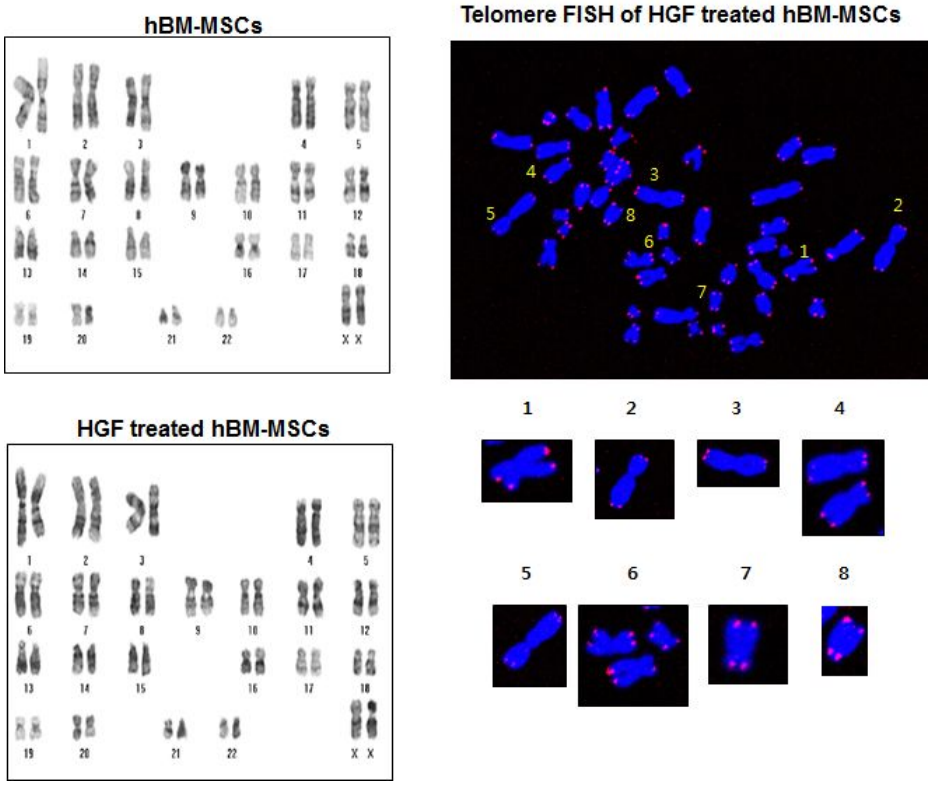
hBM-MSCs
HGF treated hBM-MSCs
Telomere FISH of HGF treated hBM-MSCs
1
2
3
4
5
6
7
8

Figure 6. HGF treatment does not adversely affect hBM-MSC genomic integrity.

(A) Expression of RAD51 and the DNA damage response marker γ-H2AX, as visualized by immunocytochemistry. UV irradiation induced the expression of γ-H2AX and RAD51; HGF treatment increased RAD51 levels but γ-H2AX was not expressed.

(B) Evaluation of chromosome stability by G-band and telomere FISH. rhHGF treatment did not affect genomic integrity in hBM-MSCs, as determined by karyotyping and telomere analyses.

Figure 7A.

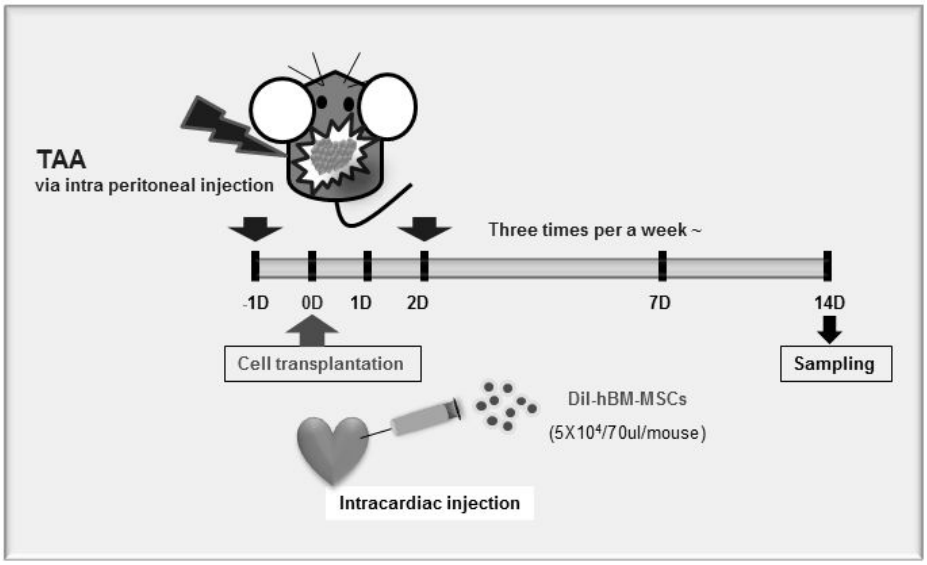
TAA-induced fibrosis mice model
TAA
via intra peritoneal injection
Three times per a week ~
-1D
0D
1D
2D
7D
14D
Cell transplantation
Sampling
DiI-hBM-MSCs
(5X10⁴/70ul/mouse)
Intracardiac injection

Figure 7B.

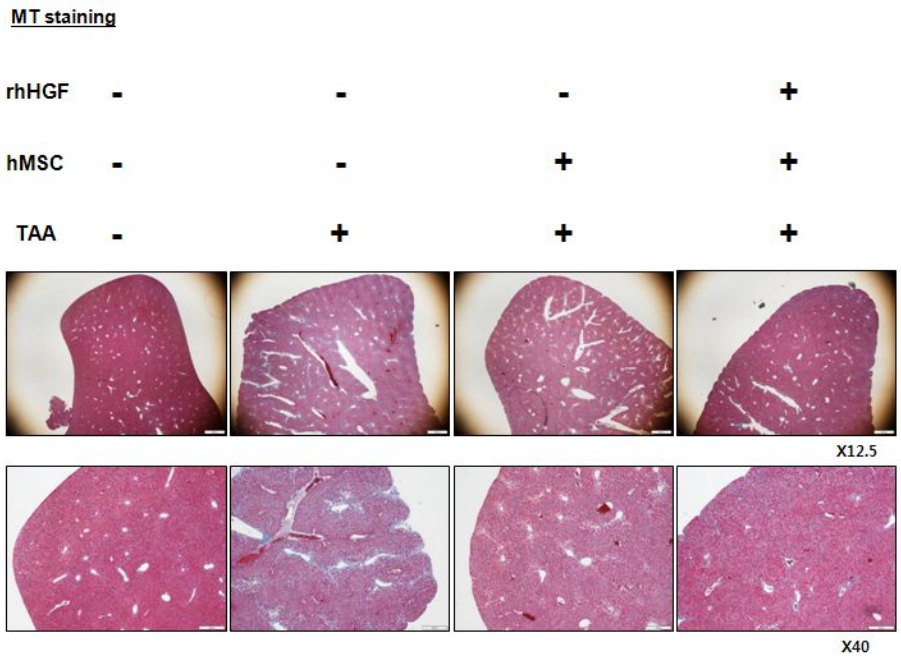

Figure 7C.

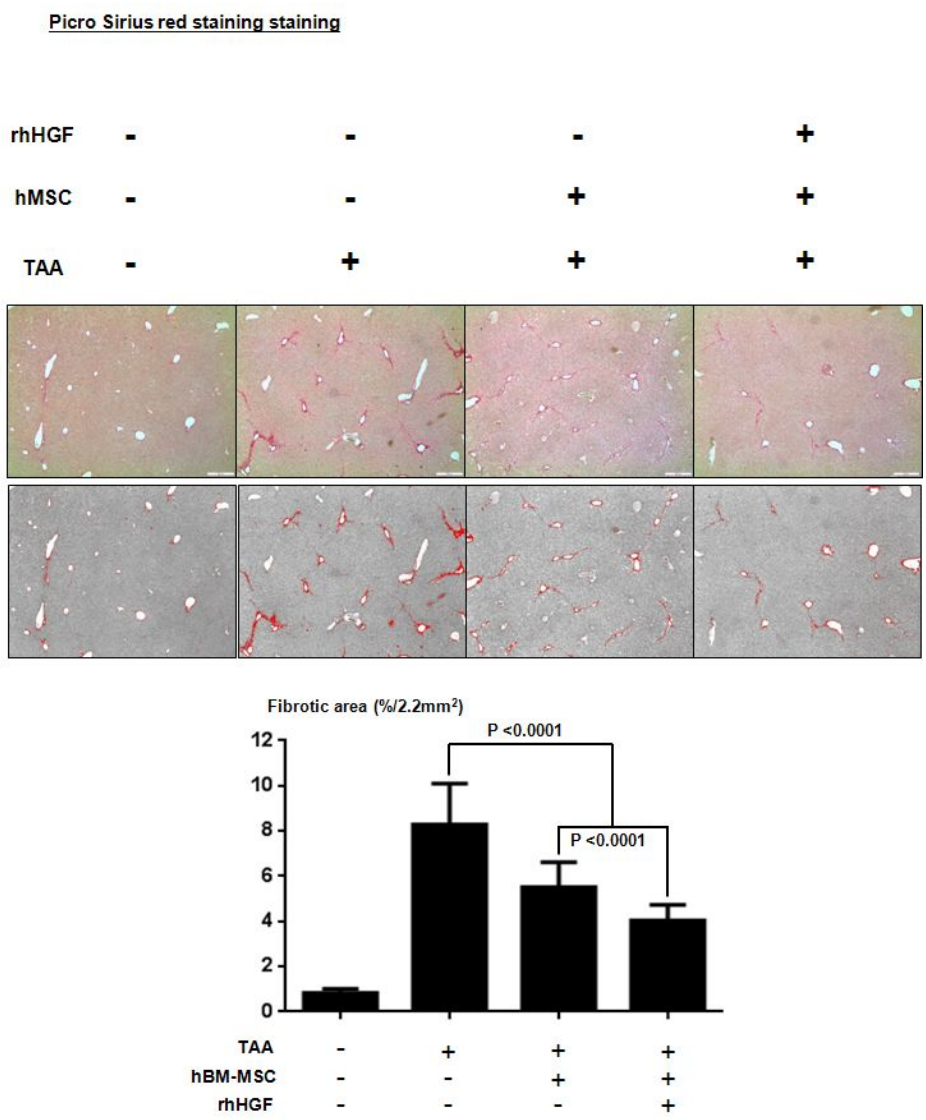
Picro Sirius red staining staining
rhHGF - - - +
hMSC - - + +
TAA - + + +
Fibrotic area (%/2.2mm²)
P <0.0001
P <0.0001
12
10
8
6
4
2
0
TAA - + + +
hBM-MSC - - + +
rhHGF - - - +

Figure 7D.

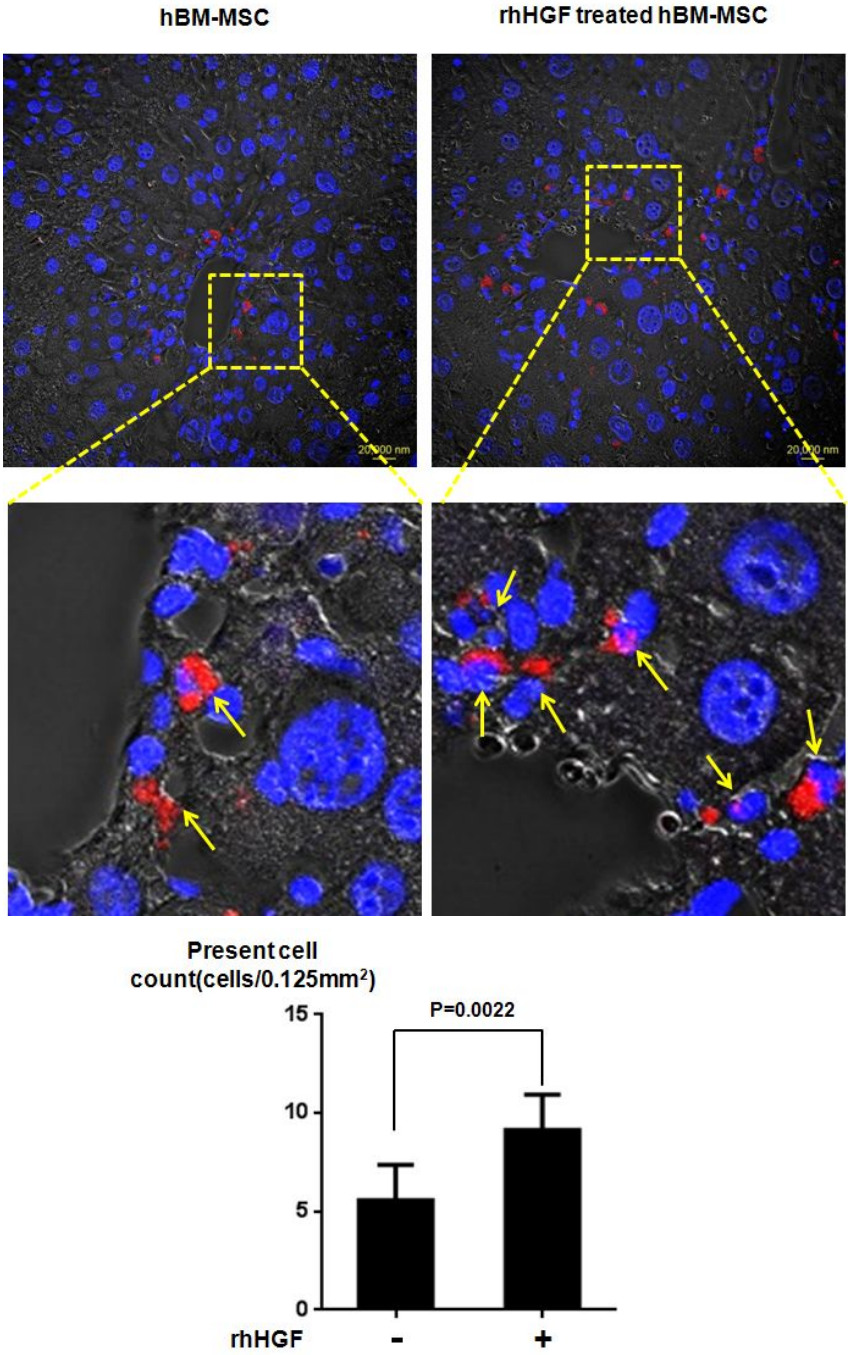
hBM-MSC
rhHGF treated hBM-MSC
Present cell count(cells/0.125mm²)
P=0.0022
15
10
5
0
rhHGF
-
+

Figure 7. HGF treatment enhances the therapeutic efficacy of hBM-MSCs.

(A) Transplantation of rhHGF-treated hBM-MSCs into the liver by intracardiac injection in a mouse model of TAA-induced liver fibrosis.

(B) Fibrotic area by Masson's trichrome staining. On day 14 post-transplantation, recovery was greater in livers transplanted with rhHGF-treated than with control hBM-MSCs, including a reduction in surface undulations.

(C) Picrosirius Red staining shows a reduction in fibrotic areas in livers transplanted with rhHGF-treated hBM-MSCs relative to control groups on day 14.

(D) DiI-labeled hBM-MSCs were counted in liver tissues at 14 days after systemic administration. The efficiency of homing, engraftment, or survival of hBM-MSC was improved by rhHGF-treatment

Supplementary Figure 1

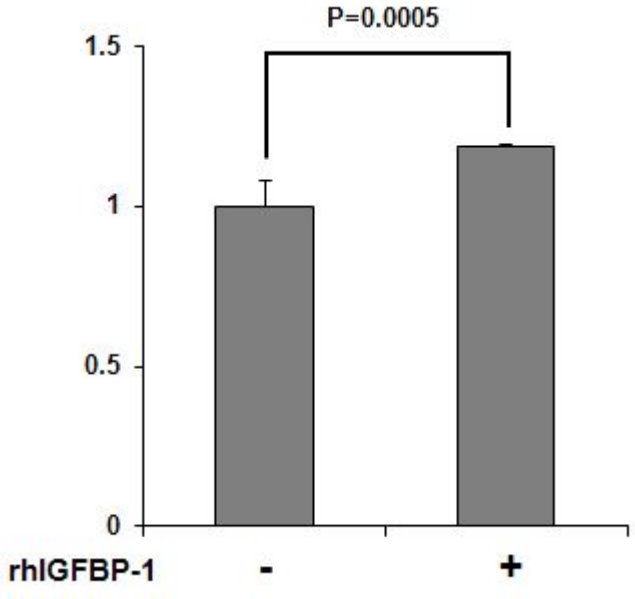

Supplementary Figure 1.

Measurement of relative telomere length (RTL) by RT-PCR. hBM-MSCs treated with rhIGFBP1 (10 ng/ml) for 5 days showed no significant changes in RTL.

Supplementary Figure 2A.

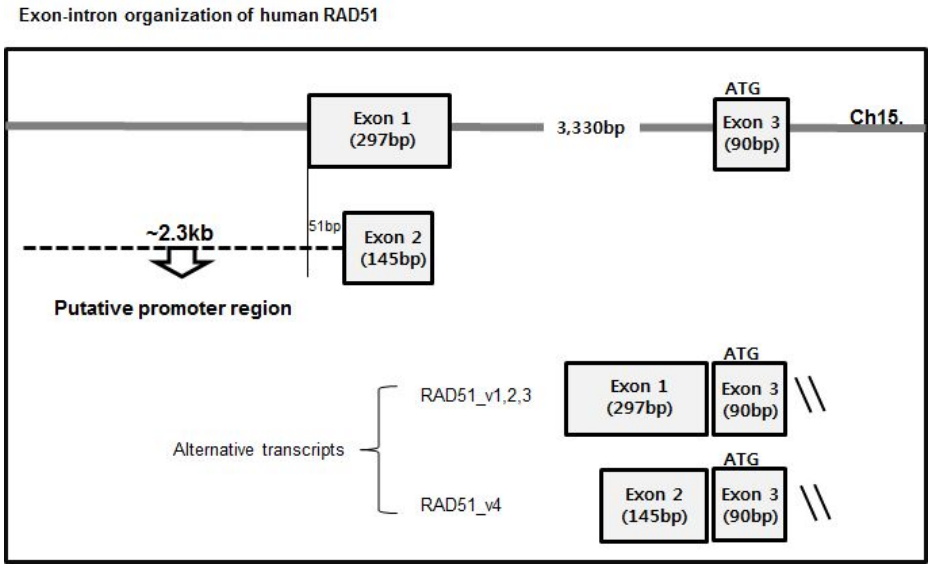

Supplementary Figure 2B.

Supplementary Figure 2.

(A) Exon-intron organization of human *RAD51*. Four alternative *RAD51* transcripts are shown, and the putative promoter region is highlighted.

(B) Screen for transcriptional activators of RAD51. IKZF1- and RUNX1-binding sites were identified with the TFSEARCH V1.3 database.

References

1. Aguilera, A., and Gomez-Gonzalez, B. (2008). Genome instability: a mechanistic view of its causes and consequences. Nat Rev Genet *9*, 204-217.
2. Bataller, R., and Brenner, D.A. (2005). Liver fibrosis. Journal of Clinical Investigation *115*, 209-218.
3. Baxter, M.A., Wynn, R.F., Jowitt, S.N., Wraith, J.E., Fairbairn, L.J., and Bellantuono, I. (2004). Study of telomere length reveals rapid aging of human marrow stromal cells following in vitro expansion. Stem cells *22*, 675-682.
4. Bertolo, A., Mehr, M., Janner-Jametti, T., Graumann, U., Aebli, N., Baur, M., Ferguson, S.J., and Stoyanov, J.V. (2013). An in vitro expansion score for tissue-engineering applications with human bone marrow-derived mesenchymal stem cells. J Tissue Eng Regen Med.
5. Filippo, J.S., Sung, P., and Klein, H. (2008). Mechanism of eukaryotic homologous recombination. Annu Rev Biochem *77*, 229-257.
6. Fuchs, E., and Chen, T. (2013). A matter of life and death: self-renewal in stem cells. Embo Rep *14*, 39-48.
7. Hasselbach, L., Haase, S., Fischer, D., Kolberg, H.C., and Sturzbecher, H.W. (2005). Characterisation of the promoter region of the human DNA-repair gene Rad51. Eur J Gynaecol Oncol *26*, 589-598.

8. Hine, C.M., Seluanov, A., and Gorbunova, V. (2008). Use of the Rad51 promoter for targeted anti-cancer therapy. Proceedings of the National Academy of Sciences of the United States of America *105*, 20810-20815.
9. Huang, C.E., Hu, F.W., Yu, C.H., Tsai, L.L., Lee, T.H., Chou, M.Y., and Yu, C.C. (2014). Concurrent Expression of Oct4 and Nanog Maintains Mesenchymal Stem-Like Property of Human Dental Pulp Cells. International journal of molecular sciences *15*, 18623-18639.
10. Inui, T., Shinomiya, N., Fukasawa, M., Kobayashi, M., Kuranaga, N., Ohkura, S., and Seki, S. (2002). Growth-related signaling regulates activation of telomerase in regenerating hepatocytes. Experimental cell research *273*, 147-156.
11. Kang, S.K., Putnam, L., Dufour, J., Ylostalo, J., Jung, J.S., and Bunnell, B.A. (2004). Expression of telomerase extends the lifespan and enhances osteogenic differentiation of adipose tissue-derived stromal cells. Stem cells *22*, 1356-1372.
12. Kim, T.M., Ko, J.H., Hu, L.C., Kim, S.A., Bishop, A.J.R., Vijg, J., Montagna, C., and Hasty, P. (2012). RAD51 Mutants Cause Replication Defects and Chromosomal Instability. Molecular and cellular biology *32*, 3663-3680.
13. Kim, W., Barron, D.A., Martin, R.S., Chan, K.S., Tran, L.L., Yang, F., Ressler, S.J., and Rowley, D.R. (2014). RUNX1 is essential for mesenchymal stem cell proliferation and myofibroblast differentiation. Proceedings of the National

Academy of Sciences of the United States of America *111*, 16389-16394.

14. Lacaud, G., Gore, L., Kennedy, M., Kouskoff, V., Kingsley, P., Hogan, C., Carlsson, L., Speck, N., Palis, J., and Keller, G. (2002). Runx1 is essential for hematopoietic commitment at the hemangioblast stage of development in vitro. Blood *100*, 458-466.
15. Lee, E.J., Choi, E.K., Kang, S.K., Kim, G.H., Park, J.Y., Kang, H.J., Lee, S.W., Kim, K.H., Kwon, J.S., Lee, K.H., et al. (2012). N-cadherin Determines Individual Variations in the Therapeutic Efficacy of Human Umbilical Cord Blood-derived Mesenchymal Stem Cells in a Rat Model of Myocardial Infarction. Molecular Therapy *20*, 155-167.
16. Lee, E.J., Lee, H.N., Kang, H.J., Kim, K.H., Hur, J., Cho, H.J., Lee, J., Chung, H.M., Cho, J., Cho, M.Y., et al. (2010). Novel Embryoid Body-Based Method to Derive Mesenchymal Stem Cells from Human Embryonic Stem Cells. Tissue Eng Pt A *16*, 705-715.
17. Lu, R., Pal, J., Buon, L., Nanjappa, P., Shi, J., Fulciniti, M., Tai, Y.T., Guo, L., Yu, M., Gryaznov, S., et al. (2014). Targeting homologous recombination and telomerase in Barrett's adenocarcinoma: impact on telomere maintenance, genomic instability and tumor growth. Oncogene *33*, 1495-1505.
18. Parekkadan, B., and Milwid, J.M. (2010). Mesenchymal Stem

Cells as Therapeutics. Annu Rev Biomed Eng *12*, 87-117.

19. Price, B.D., and D'Andrea, A.D. (2013). Chromatin Remodeling at DNA Double-Strand Breaks. Cell *152*, 1344-1354.
20. Samsonraj, R.M., Raghunath, M., Hui, J.H., Ling, L., Nurcombe, V., and Cool, S.M. (2013). Telomere length analysis of human mesenchymal stem cells by quantitative PCR. Gene *519*, 348-355.
21. Shi, S.T., Gronthos, S., Chen, S.Q., Reddi, A., Counter, C.M., Robey, P.G., and Wang, C.Y. (2002). Bone formation by human postnatal bone marrow stromal stem cells is enhanced by telomerase expression. Nat Biotechnol *20*, 587-591.
22. Simonsen, J.L., Rosada, C., Serakinci, N., Justesen, J., Stenderup, K., Rattan, S.I.S., Jensen, T.G., and Kassem, M. (2002). Telomerase expression extends the proliferative life-span and maintains the osteogenic potential of human bone marrow stromal cells. Nat Biotechnol *20*, 592-596.
23. Stewart, S.A., Ben-Porath, I., Carey, V.J., O'Connor, B.F., Hahn, W.C., and Weinberg, R.A. (2003). Erosion of the telomeric single-strand overhang at replicative senescence. Nat Genet *33*, 492-496.
24. Takeuchi, M., Takeuchi, K., Kohara, A., Satoh, M., Shioda, S., Ozawa, Y., Ohtani, A., Morita, K., Hirano, T., Terai, M., et al. (2007). Chromosomal instability in human mesenchymal stem cells immortalized with human papilloma virus E6, E7, and hTERT genes (vol 43, pg 129, 2007). In Vitro Cell Dev-An

43, 315-318.

25. Tarsounas, M., Munoz, P., Claas, A., Smiraldo, P.G., Pittman, D.L., Blasco, M.A., and West, S.C. (2004). Telomere maintenance requires the RAD51D recombination/repair protein. Cell *117*, 337-347.
26. Tsai, C.C., Su, P.F., Huang, Y.F., Yew, T.L., and Hung, S.C. (2012). Oct4 and Nanog directly regulate Dnmt1 to maintain self-renewal and undifferentiated state in mesenchymal stem cells. Molecular cell *47*, 169-182.
27. Wang, J., Hannon, G.J., and Beach, D.H. (2000). Cell biology - Risky immortalization by telomerase. Nature *405*, 755-756.
28. Yoshida, T., Landhuis, E., Dose, M., Hazan, I., Zhang, J.W., Naito, T., Jackson, A.F., Wu, J., Perotti, E.A., Kaufmann, C., et al. (2013). Transcriptional regulation of the Ikzf1 locus. Blood *122*, 3149-3159.

국문초록

인간 배아 줄기 세포 유래 중간엽 줄기 세포 (hE-MSCs)는 세포 기반 치료를 위한 성체 줄기 세포보다 더 나은 대안을 나타낼 수 있습니다. 중배엽 줄기 세포를 젊어지게 하는 factor를 개발하기 위해, 우리는 hE-MSC에서 더 강하게 발현된 cytokine을 이용하여 hE-MSC와 성체 줄기 세포(hBM-MSC)를 비교하였다. 우리는 hE-MSC와 hBM-MSC의 기능 상실, 획득 실험을 통해 간세포 성장인자 (HGF)를 확인했다. hBM-MSC에 HGF의 첨가하여 Telomere의 길이의 증가와 Oct4 및 Nanog를 발현 증가를 보았다. 다음으로, 우리는 telomere 하위의 최대 조절자로 HGF로 RAD51을 확인했다. Oct4 및 Nanog는 hBM-MSC에서 RAD51 과발현에 의해 상향 조절 및 RAD51의 siRNA에 의해 하향 조절했다. 우리는 RAD51의 추정 프로모터를 상영 IKZF과 RUNX1에 대한 결합 부위 전사를 확인했다. hBM-MSC에서 IKZF과 RUNX1의 발현을 억제하고, 제조합 인간 간세포 성장인자(rhHGF)를 처리하여도 telomere의 길이가 짧아지고, Oct4, Nanog,뿐만 아니라 RAD51 발현을 감소시켰다. 마지막으로 우리는 중배엽 줄기 세포에서 rhHGF의 안전을 확인했다. G-band와 telomere의 FISH는 정상 염색체로 확인하였으며, TAA에 의한 간 섬유화 쥐 모델은 hBM-MSC의 rhHGF 처리에 따라 질량을 형성하지 않고 치료 증가 효과를 보였다.

주요어 : 인간배아줄기세포유래 중배엽 줄기 세포, 인간 골수 유래 중배엽 줄기 세포, 간세포 성장인자, 라드51

학번 : 2013-24032